

Verification of polarization selection rules and implementation of selective coherent manipulations of hydrogenic transitions in n-GaAs

M. F. Doty, B. T. King, and M. S. Sherwin*

*California Nanosystems Institute and Institute for Quantum Engineering, Science, and Technology,
University of California, Santa Barbara. Santa Barbara, California 93106*

C. R. Stanley

*Department of Electronics and Electrical Engineering,
University of Glasgow, Glasgow, G12 8QQ, UK*

(Dated: June 22, 2021)

Electrons bound to shallow donors in GaAs have orbital energy levels analogous to those of the hydrogen atom. The polarization selection rules for optical transitions between the states analogous to the 1s and 2p states of hydrogen in a magnetic field are verified using Terahertz (THz) radiation from the UCSB Free Electron Laser. A polarization-selective coherent manipulation of the quantum states is demonstrated and the relevance to quantum information processing schemes is discussed.

In recent years there has been great interest in low dimensional semiconductors, motivated in large part by the potential to implement quantum information processing^{1,2,3} in a solid-state system^{4,5,6}. The development of methods for selectively addressing and coherently manipulating such quantum systems is essential to a successful implementation of any quantum information scheme. In this work we describe verification of the selection rules for orbital transitions of electrons bound to shallow donors in GaAs and implementation of selective coherent manipulations.

The energy levels of shallow donor-bound electrons can be described by the Coulomb interaction between the electron and the positive charge at the donor site, modified by the effective mass of the electron (0.0665 m_e) and the dielectric constant of the material (12.56)^{7,8}. This leads to electron energy levels analogous to those of the hydrogen atom, with a small correction for the actual donor species, called the central cell correction (0.110 meV for S donor)⁹. The orbital transitions are in the TeraHertz (THz) frequency regime (a few meV). In the presence of a magnetic field, additional free electron states arise, forming a continuum above each Landau level⁸. The hydrogenic states can be labelled with the usual notation: 1s, 2p⁺, 2p⁻, etc.

The energy of the hydrogenic states can be tuned with an applied magnetic field to bring orbital transitions into resonance with fixed frequencies of radiation. Klaassen, et al.⁸ and Stillman, et al.¹⁰, have used this technique to perform spectroscopy experiments. To aid in identifying excited states, they have assumed that transitions are governed by the usual hydrogen atom dipole selection rules. However, these experiments have not included control of the polarization state of the THz beam, and to our knowledge no work has yet verified that the hydrogen selection rules remain valid for hydrogenic donors in a semiconductor.

The hydrogen selection rules require a σ^+ -polarized photon to conserve angular momentum and excite the 1s to 2p⁺ transition; σ^- -polarization is required for 1s

to 2p⁻. Since the electron effective mass in GaAs is isotropic, the selection rules for the bare hydrogen atom might be expected to hold. However, symmetry in a semiconductor can easily be lost. In quantum dots, for example, elongation of the dot along specific crystal planes can break the dot symmetry and mix the polarization eigenstates of excitons¹¹. In this work, we first verify the selection rules for the 1s to 2p[±] transitions by varying the polarization of the incident THz radiation. We then utilize the rules to demonstrate a selective coherent manipulation of orbital energy states.

The sample studied was grown by Molecular Beam Epitaxy (MBE) with a 15- μ m layer of unintentionally-doped GaAs on top of a semi-insulating GaAs substrate. The donor density is $2.8 \times 10^{14} \text{ cm}^{-3}$, determined by measuring the Hall resistance, and sulfur is the dominant impurity. A 200 nm silicon-doped capping layer was grown on top of the sample to facilitate Ohmic contacts, and was etched away from the active area of the sample ($50 \times 50 \mu\text{m}^2$). All experiments were done with the sample immersed in liquid helium at 1.5 K in a magneto-optical cryostat. At this temperature, the electrons are initially in the ground state (1s). Electrons in bound excited states, which have an increased probability of thermal excitation to the conduction band, are detected by applying a 50 mV bias and measuring the transient photoconductivity. The recapture of conduction band electrons occurs much more rapidly than the repetition rate of our laser ($\sim 1 \text{ Hz}$), and so the electrons return to the ground state before any subsequent excitation.

The UCSB Free Electron Laser (FEL) provides linearly polarized THz radiation for our experiments. Three different THz frequencies in bands of low atmospheric absorption are used and the hydrogenic states are tuned into resonance with the radiation using the magnetic field. Fig. 1 shows the energy of the 1s and 2p states as a function of magnetic field, as well as the lowest Landau levels.

Before illuminating the sample, the THz radiation is reflected off a wire-grid polarizer (rotated by 45 degrees

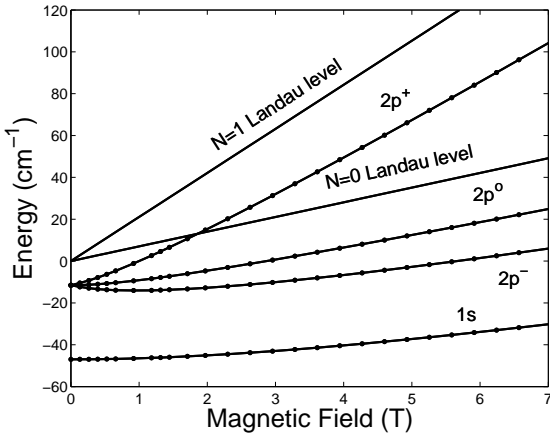


FIG. 1: The energy levels of the 1s and 2p hydrogenic states and the lowest two Landau levels as a function of magnetic field. The lowest Landau level at zero magnetic field has been taken to be zero energy. The points are taken from the calculations of Makado and McGill¹³ and are converted from dimensionless units using constants given by Klaassen, et al.⁸ The central cell correction has been added following the work of Heron, et al.⁹ The lines are drawn through the points.

with respect to the incident electric field) followed by a mirror. The total reflected beam consists of two orthogonal, linearly-polarized components of equal amplitude, with a phase delay controlled by the mirror-polarizer spacing. Varying this spacing varies the polarization of the light incident on the sample. The metal contacts on the sample (identical to that used by Cole, et al.¹⁴) are designed to minimize distortions of the incident polarization.

The output polarization state of the light is quantified using the Stokes parameters: S_0 - S_3 . S_0 , S_1 and S_2 can be determined from simple measurements of transmission through an analyzer as measured with a polarization-insensitive detector, in our case an InSb hot-electron bolometer. The magnitude of S_3 can be determined from the relation

$$S_0^2 = S_1^2 + S_2^2 + S_3^2$$

and the sign can be determined by knowing the spacing of the mirror-polarizer combination with respect to a fixed direction of linear polarization. The ratio S_3/S_0 is +1 for perfectly σ^+ -polarized light and -1 for perfectly σ^- -polarized light.

To verify the selection rules, the sample is illuminated with a long ($\sim 5 \mu\text{s}$) pulse of THz radiation and the photoconductivity is plotted as a function of mirror-polarizer spacing. The photoconductivity under long-pulse illumination of this sample always shows a saturation-like behavior as a function of intensity. See Fig. 2a for an example. All data on selection rules is taken with sufficient attenuation to be in the low-intensity quasi-linear regime.

Fig. 2b-d shows the photocurrent as a function of

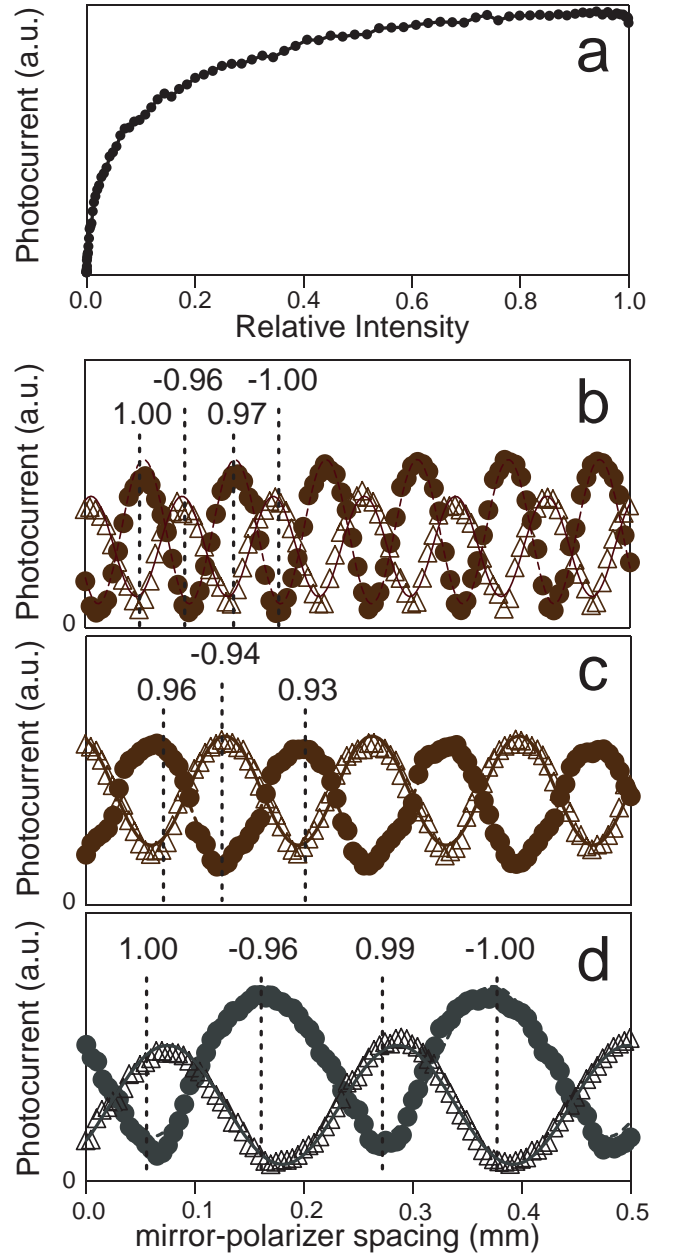


FIG. 2: (a) Photocurrent versus relative intensity (varied with crossed polarizers) of a $5\text{-}\mu\text{s}$ pulse of radiation at 1.07 THz. (b-d) Photocurrent as a function of micrometer spacing (proportional to phase delay). Circles correspond to a field oriented in the $+z$ direction, triangles to $-z$. The size of the symbols is chosen to represent the error bars. The solid and dashed lines are fits to the data using a sine function. The vertical cut lines indicate the polarization state of the light (S_3/S_0) measured at that spacing. (b) The 1s to $2p^+$ transition at 2.53 THz and $B = 3.63$ T. (c) The 1s to $2p^+$ transition at 1.57 THz and $B = 1.38$ T. (d) The 1s to $2p^-$ transition at 1.01 THz and $B = 3.5$ T.

the mirror-polarizer spacing. As expected, the photocurrent varies with the spacing (polarization of the incident light). The period of the variation in photocurrent is determined by the change in mirror-polarizer spacing that corresponds to a one-wavelength path-length difference. To verify that the change in photocurrent is due only to the selection rules, the experiment is repeated with the magnetic field oriented in the $+z$ (circles) and $-z$ (triangles) direction.

For Fig. 2b and 2c, the maximum photocurrent obtained with the magnetic field in the $+z$ direction (circles) corresponds to σ^+ -polarized light, the expected handedness for the $1s$ to $2p^+$ transition. For Fig. 2d, exciting the $2p^-$ transition, the maximum photocurrent corresponds to σ^- -polarized light. For all three cases, it is clear that the handedness of polarization that excites the transition reverses when the static magnetic field is reversed (triangles), in agreement with the hydrogen atom selection rules. The sine curves fit to the data for the anti-parallel directions of the magnetic field should have phases that differ by π . The measured phase differences in radians are (b) 3.63, (c) 3.13 and (d) 3.57. Slight distortion of the incident polarization (from the focusing element and cryostat windows) is the most likely source of the offset from zero photoconductivity. Near-resonant excitation of other transitions may also be contributing. The difference in maximum signal for the two opposed directions of the magnetic field is not understood.

The selection rules are now used to perform a selective coherent state transition. By “selective transition” we mean that a coherent manipulation (Rabi oscillation) of the two-level quantum system is turned on or off by varying only the polarization state of the incident light. To drive a Rabi oscillation, short, intense pulses of THz radiation with a controllable pulse width are generated. The short pulses are extracted from the high-intensity long-pulse output of the UCSB FEL with laser-activated semiconductor switches.^{15,16} The switches are manufactured from silicon and are activated by illumination with near-infrared radiation across the band gap, which generates a reflecting electron-hole plasma.¹⁷ Step-function-like activation of the switches is obtained with a very short (~ 150 fs), intense (> 1 mJ per switch) near-infrared pulse. The switches are arranged in a reflection (the reflected light is kept in the optical path) and transmission (the reflected light is dumped) geometry. By varying the arrival of the activation pulse at the reflection and transmission switches, the width of the THz pulse is controlled.

No attenuation is used for the short pulse experiment since coherent manipulations require strong coupling. A “stroboscopic” measurement, in which the photocurrent is plotted as a function of the pulse width, is performed to get a map of the electron state population as a function of time. This method was used by Cole, et al.¹⁴, who first demonstrated a coherent manipulation of the orbital states of hydrogenic donors.

Data showing a selective coherent manipulation between the $1s$ and $2p^+$ states is presented in Fig. 3. A

vertical offset has been added to separate the traces. The upper trace was obtained using σ^+ -polarized light; at pulse widths of about 15 ps excited electrons are being driven back into the ground ($1s$) state before they can ionize and so a decrease in the photocurrent is observed, the signature of a Rabi oscillation. For horizontally-polarized (π_x) and vertically-polarized (π_y) light, a Rabi oscillation is still visible, but the period of the oscillation is longer (20-25 ps) since only half of the linearly-polarized light couples in to the transition. Small errors in the mirror-polarizer spacing probably caused the difference in oscillation period between the horizontally- and vertically-polarized data. When the polarization is changed to σ^- there is no evidence of a Rabi oscillation. There is a shallow increase in photoconductivity, which we attribute to a non-zero σ^+ component of the polarization arising from the coupling in to the cryostat, as described above.

Information about the dynamics of the electrons can be extracted from this data by fitting to a theoretical model. The density-matrix equations of motion for a two-level system are used, with damping processes added¹⁸. The equations are

$$\begin{aligned}\rho_{11} &= \frac{1}{2}i\Omega_R\sigma_{12} - \frac{1}{2}i\Omega_R\sigma_{21} + \Gamma_1\rho_{22} \\ \rho_{22} &= -\frac{1}{2}i\Omega_R\sigma_{12} + \frac{1}{2}i\Omega_R\sigma_{21} - \Gamma_1\rho_{22} - \gamma_3\rho_{22} \\ \sigma_{12} &= -i(\omega - \omega_0)\sigma_{12} + \frac{1}{2}i\Omega_R(\rho_{11} - \rho_{22}) - \gamma_2\sigma_{12}\end{aligned}$$

where ρ_{11} and ρ_{22} are proportional to the populations of the $1s$ and $2p^+$ states, respectively. σ_{12} and $\sigma_{21} (= \sigma_{12}^*)$ are related to the phase coherence of the ensemble and are obtained by finding slowly-varying solutions in the rotating wave approximation. $\Omega_R = eE_{THz}x_{12}/\hbar$ is the Rabi frequency, with e the electric charge, E_{THz} the THz electric field amplitude, and x_{12} the dipole matrix element. The damping terms are: Γ_1 , the rate of recombination from the $2p^+$ to the $1s$ state (inverse lifetime); γ_2 , the dephasing rate of the ensemble and γ_3 , the rate of ionization from the $2p^+$ state into the conduction band. ω is the frequency of the driving THz field and ω_0 is the resonant frequency for the transition.

This model is fit to the data under the assumption that the driving field is on resonance ($\omega - \omega_0 = 0$) and the recombination rate is zero ($\Gamma_1 = 0$). The second assumption is known to be valid since the recombination rate is much slower than the other damping processes. The photoconductivity is taken to be equal to $1 - \rho_{11}(t)$ since the $2p^+$ state lies within the conduction band and all electrons excited out of the ground state are expected to arrive in the conduction band within our probing window. The solid lines in Fig. 3 show the results of the fits. The fit to the σ^+ data yields the values $\gamma_2 = 1.98 \times 10^{11} \text{ s}^{-1}$ and $\gamma_3 = 1.22 \times 10^{11} \text{ s}^{-1}$. These values correspond to a dephasing time of 5 ps and ionization time of 8 ps. Considerably longer dephasing and ionization times were reported by Cole, et al.¹⁴ for illumination with lower inten-

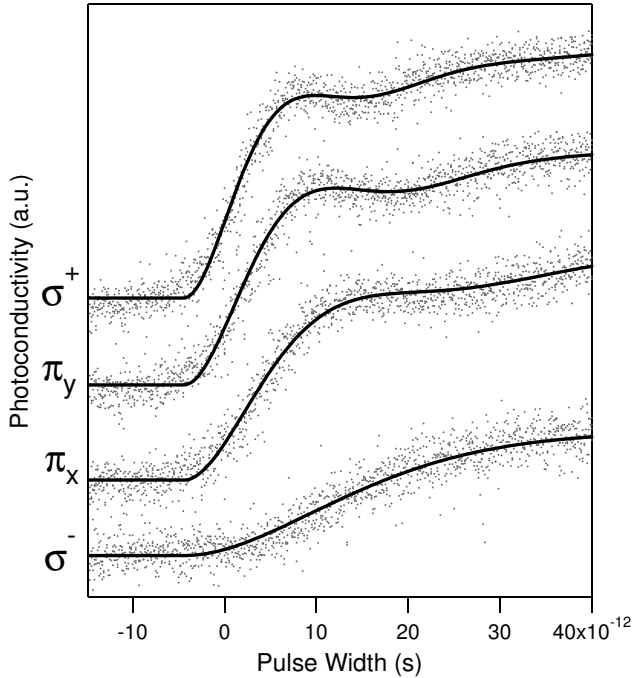


FIG. 3: Photoconductivity versus pulse width using different polarizations. The illumination frequency is 84.5 cm^{-1} (2.54 THz) and the magnetic field is 3.62 T. The solid lines are fits to the data using the model described in the text.

sities of THz radiation. The longer damping time arises because the dominant damping process is associated with coupling to the conduction band states, as described by Brandi, et al.¹⁹. Lower intensities result in slower excita-

tion to the conduction band and thus slower contribution of this extrinsic damping.

In summary, the selection rules for hydrogenic transitions in n-GaAs have been verified by monitoring the photocurrent, which is generated by ionization of the bound excited state population, as a function of incident polarization. These selection rules can be used to determine the required electric fields in the design of a THz cavity to couple hydrogenic states of different donors. A THz photonic cavity, which is significantly larger than an equivalent visible-frequency cavity, would facilitate spatial addressing of individual donors in a quantum information processing scheme⁶.

Using short, intense pulses of THz radiation polarized in compliance with the selection rules, Rabi oscillations were driven between orbital energy states. The absence of a Rabi oscillation when illuminating with high-intensity but incorrectly-polarized radiation demonstrates a selective state manipulation. Polarized radiation that coupled specific states was used by Li, et al. to demonstrate a quantum logic gate using excitons in a single quantum dot.¹² The selective coherent manipulation presented in this work is a first step toward the implementation of more complex quantum logic operations using donor-bound electrons.

Acknowledgments

The authors wish to acknowledge the assistance of David Enyeart in the operation of the UCSB FEL. This work was supported by the DARPA QuIST program under Grant No. MDA972-01-1-0027 and by SUN microsystems.

- * Electronic address: sherwin@physics.ucsb.edu
- ¹ C. H. Bennett and D. P. DiVincenzo, *Nature* **404**, 247 (2000).
- ² N. A. Gershenfeld and I. L. Chuang, *Science* **275**, 350 (1997).
- ³ J. I. Cirac and P. Zoller, *Phys. Rev. Lett* **74**, 4091 (1995).
- ⁴ A. Imamoglu, D. D. Awschalom, G. Burkard, D. P. DiVincenzo, D. Loss, M. Sherwin, and A. Small, *Phys. Rev. Lett.* **83**, 4204 (1999).
- ⁵ E. Biolatti, R. C. Iotti, P. Zanardi, and F. Rossi, *Phys. Rev. Lett.* **85**, 5647 (2000).
- ⁶ M.S. Sherwin, A. Imamoglu, and T. Montroy, *Phys. Rev. A* **60**, 3508 (1999).
- ⁷ W. Kohn, *Solid State Physics: Advances in Research and Applications* **5**, 257 (1957).
- ⁸ Tjeerd O. Klaassen, Janette L. Dunn, and Colin A. Bates, in *Atoms and Molecules in Strong External Fields*, edited by Schmelcher and Schweizer (Plenum Press, 1998), pp. 291–300.
- ⁹ R.J. Heron, R.A. Lewis, P.E. Simmonds, R.P. Starrett, A.V. Skougarevsky, R.G. Clark, and C.R. Stanley, *Journal of Applied Physics* **85**, 893 (1999).
- ¹⁰ G.E. Stillman, C.M. Wolfe, and J.O. Dimmock, *Solid State*

- Communications
- ¹¹ T. H. Stievater, X. Li, T. Cubel, D. G. Steel, D. Gammon, D. S. Katzer, and D. Park, *App. Phys. Lett.* **81**, 4251 (2002).
- ¹² X. Li, Y. Wu, D. Steel, D. Gammon, T. H. Stievater, D. S. Katzer, D. Park, C. Piermarocchi, and L. J. Sham, *Science* **301**, 809 (2003).
- ¹³ P.C. Makado and N.C. McGill, *J. Phys. C: Solid State Phys.* **19**, 873 (1986).
- ¹⁴ B.E. Cole, J.B. Williams, B.T. King, M.S. Sherwin, and C.R. Stanley, *Nature* **410**, 60 (2001).
- ¹⁵ F. A. Hegmann and M. S. Sherwin, in *International conference on millimeter and submillimeter waves and applications III*. (SPIE, 1996).
- ¹⁶ F. A. Hegmann, J. B. Williams, B. Cole, M. S. Sherwin, J. W. Beeman, and E. E. Haller, *Appl. Phys. Lett.* **76**, 262 (2000).
- ¹⁷ M. F. Doty, B. E. Cole, B. T. King, and M. S. Sherwin, *Rev. Sci. Inst.* **75**, 2921 (2004).
- ¹⁸ R. W. Boyd, *Nonlinear Optics* (Academic Press, 1992).
- ¹⁹ H.S. Brandi, A. Latge, and L.E. Oliveira, *Phys. Rev. B* **68**, 233206 (2003).